Pharmacokinetics and Pharmacodynamic Effects of Nemvaleukin Alfa, a Selective Agonist of the Intermediate-Affinity IL-2 Receptor, in Cynomolgus Monkeys*

Jared E. Lopes,[1] **Lei Sun,**[1] Heather L. Flick, Erin A. Murphy, and Heather C. Losey[2]

Affiliation:

Alkermes, Inc., Waltham, Massachusetts (J.E.L., L.S., H.L.F., E.A.M., H.C.L.)

Target journal: *Journal of Pharmacology and Experimental Therapeutics*

Running title (60-character limit, incl. spaces): Pharmacology of nemvaleukin alfa in cynomolgus monkeys

Corresponding author:

Heather C. Losey

Alkermes, Inc.

852 Winter St.

Waltham, MA 02451

Phone: 781-609-6944

E-mail: heather.losey@alkermes.com

Number of text pages: 16

Number of tables: 3

Number of figures: 4

Number of references: 25

Number of words in Abstract: 247

Number of words in Introduction: 660

Number of words in Discussion: 904

Number of Supplementary tables: 4

Number of Supplementary figures: 3

Nonstandard abbreviations: AUC, area under the concentration-time curve; AUMC, area under the moment curve; CL, total body clearance; C_{max}, maximum observed serum concentration; γ_c, common γ; IFNγ, interferon-γ; IL, interleukin; IL-2R, interleukin-2 receptor; i.v., intravenous; Mab, monoclonal antibody; MRT, mean residence time; MSD, Meso Scale Discovery; NK, natural killer; PD, pharmacodynamics; PK,

pharmacokinetics; T_{max}, time to C_{max}; T_{reg}, regulatory T cell; Vd_{ss}, volume of distribution at steady state

Recommended section assignment:

- Drug Discovery and Translational Medicine

ABSTRACT (250-word limit; currently at 247 words)

Nemvaleukin alfa (nemvaleukin, ALKS 4230) is a novel cytokine, created by the fusion of circularly permuted interleukin-2 (IL-2) to the IL-2Rα subunit of the IL-2 receptor (IL-2R) complex, that confers selectivity for the intermediate-affinity IL-2R expressed on CD8^{+} T cells and natural killer (NK) cells. The pharmacokinetics and selective pharmacodynamic properties of nemvaleukin have been demonstrated using in vitro and in vivo mouse models. The pharmacokinetic/pharmacodynamic effects of nemvaleukin on immune cell subtypes were evaluated in cynomolgus monkeys following intravenous (i.v.) and subcutaneous (s.c.) administration to inform dose selection and predict pharmacodynamic effects in humans. Male drug-naïve cynomolgus monkeys ($N = 15$) were administered either single-dose (i.v. 0.3 mg/kg; s.c. 0.3 mg/kg or 1.0 mg/kg) or repeated-doses (i.v. 0.1 mg/kg on days 1–5 or s.c. 0.5 mg/kg on days 1 and 4) of nemvaleukin. Serial blood samples were collected for pharmacokinetic assessment, immunophenotyping by flow cytometry, and profiling of serum cytokines. Repeat-dose s.c. administration of nemvaleukin with less frequent dosing resulted in total systemic exposure and trough serum concentrations comparable to those seen with i.v. administration, with lower peak serum concentrations. Transient elevation of interferon-γ and IL-6 peaked at 2 and 8 hours after i.v. and s.c. administration, respectively. Selective expansion of immunoprotective central memory, effector memory, and terminal effector CD8^{+} T cells and CD56^{+} NK cells, and minimal expansion of immunosuppressive CD4^{+}CD25^{+}FoxP3^{+} regulatory T cells was observed following both i.v. and s.c. administration. These data support the ongoing clinical evaluation of i.v. and s.c. nemvaleukin.

SIGNIFICANCE STATEMENT (80-word limit; currently at 80 words)

Administration of the novel interleukin-2 receptor agonist nemvaleukin alfa (nemvaleukin, ALKS 4230) to cynomolgus monkeys resulted in selective expansion of immune effector cells, including CD8$^+$ T and NK cells, with minimal effects on immunosuppressive CD4$^+$ regulatory T cells, confirming the design of nemvaleukin and highlighting its potential as a cancer immunotherapy. Subcutaneous administration of nemvaleukin achieved systemic exposure and immunostimulatory effects similar to those observed following more frequent intravenous dosing and may represent a practical alternative in a clinical setting.

KEYWORDS

Pharmacokinetics, pharmacodynamics, nemvaleukin alfa, cynomolgus monkeys, interleukin-2, immunotherapy

Introduction (700-word limit; currently at 687 words)

Interleukin-2 (IL-2) was originally discovered as a T cell growth factor based on its ability to promote the growth of lymphocytes in vitro (Boyman and Sprent, 2012). However, it is now appreciated that IL-2 plays a much larger role in maintaining immune homeostasis, given that it is required for the development and function of immunosuppressive $CD4^+CD25^+CD127^{low/-}FoxP3^+$ regulatory T cells ($CD4^+$ T_{regs}), as well as the function of immune effector cells, including conventional $CD4^+$ T cells, $CD8^+$ T cells, natural killer (NK) cells, and B cells (Waldmann, 2006; Boyman and Sprent, 2012; Choudhry et al., 2018). Presentation of tumor antigens by mature dendritic cells to antigen-specific $CD4^+$ and $CD8^+$ T cells in secondary lymphoid tissues results in the expression of high-affinity IL-2R complexes and the local production of IL-2, supporting the expansion of tumor antigen–specific T cells (Boyman and Sprent, 2012). NK cells, which are cytotoxic for major histocompatibility complexes class I–deficient tumor cells, also express high- and intermediate-affinity IL-2R complexes. However, high-affinity IL-2R complexes are constitutively expressed on $CD4^+$ T_{regs} (Boyman and Sprent, 2012). Thus, by activating and expanding $CD4^+$ T_{regs}, as well as conventional $CD4^+$ T cells, $CD8^+$ T cells, and NK cells, IL-2 exerts dual regulatory (eg, on immunosuppressive $CD4^+$ T_{regs}) and stimulatory (eg, on immune effector $CD8^+$ T cells and NK cells) effects on the immune cells that are integral to the cancer immunity cycle. Recombinant IL-2 (aldesleukin) was among the first immunotherapies to be approved for the treatment of advanced/metastatic renal cell carcinoma and melanoma. Paradoxically, the high doses required for antitumor activity have been associated with activation and expansion of high-affinity IL-2R–expressing $CD4^+$ T_{regs} that are hypothesized to hinder antitumor

efficacy. Furthermore, widespread use of high-dose IL-2 has been limited due to its association with potentially life-threatening acute toxicities (eg, vascular leak syndrome that can lead to liver cell damage and renal failure), which may be explained by the expression of the high-affinity IL-2R complex on endothelial cells (Atkins et al., 1999; Boyman and Sprent, 2012; Sim et al., 2014; Amaria et al., 2015; Choudhry et al., 2018).

Leveraging the immunostimulatory effects of IL-2, while at the same time mitigating the protumor activation and expansion of CD4$^+$ T$_{regs}$ and avoiding the toxicity associated with high doses, is hypothesized to enhance the immunotherapeutic potential of IL-2 (Ahmadzadeh and Rosenberg, 2006; Skrombolas and Frelinger, 2014). This strategy can be achieved through selective targeting of the intermediate-affinity IL-2R, comprising IL-2Rβ and common γ (γ$_c$) chains, expressed on immune effector cells, including CD8$^+$ T cells and NK cells, while avoiding activation of the high-affinity IL-2R, comprising IL-2Rα (also known as CD25), IL-2Rβ, and γ$_c$ chains, expressed on CD4$^+$ T$_{regs}$, and endothelial cells (Boyman and Sprent, 2012).

Nemvaleukin alfa (nemvaleukin, ALKS 4230) is a novel, engineered cytokine that was created by fusing circularly permuted IL-2 to the extracellular domain of the IL-2Rα subunit of the IL-2R complex (Fig. 1A). In comparison with IL-2, nemvaleukin selectively engages the intermediate-affinity IL-2R complex that is expressed on subsets of CD8$^+$ T cells and NK cells and is sterically occluded from binding to the high-affinity IL-2R complex that is expressed preferentially on CD4$^+$ T$_{regs}$ (Fig. 1B) (Antony and Restifo, 2005; Sun et al., 2019; Lopes et al., 2020). Data from in vitro human studies and in vivo mouse studies have shown that, compared with recombinant human IL-2, nemvaleukin selectively activates and expands circulating NK cells and memory-phenotype CD8$^+$ T

cells, with negligible effects on CD4$^+$ T$_{regs}$ (Lopes et al., 2020). This selective expansion of immune effector cells with antitumor function(s) has promising therapeutic potential, and clinical studies of nemvaleukin, as monotherapy or in combination with the anti–programmed death-1 checkpoint inhibitor pembrolizumab, in patients with advanced solid tumors are ongoing (ARTISTRY-1 [NCT02799095]; ARTISTRY-2 [NCT03861793]; ION-01 nemvaleukin [NCT04144517]).

The present study examines the pharmacokinetics (PK) and pharmacodynamic (PD) effects of nemvaleukin on multiple immune cell subtypes (including circulating CD8$^+$ T cells, NK cells, CD4$^+$ T cells, and CD4$^+$ T$_{regs}$) in cynomolgus monkeys following intravenous (i.v.) and subcutaneous (s.c.) routes of administration. The PK-PD relationship in cynomolgus monkeys is expected to inform dose selection and predict PD effects in humans.

Materials and Methods

Animals

Male drug-naïve cynomolgus monkeys (N = 15) [Covance Laboratories, Inc (Madison, WI) and Covance Research Products, Inc. (Alice, TX)] aged 2–4 years were housed in stainless steel cages at ambient temperatures under a 12-hour light/dark cycle and fed a certified primate diet with water ad libitum. Following acclimation to study conditions over a 1- to 4-day period, animals were selected for testing based on their overall health and body weight, which ranged from 2.4 kg to 3.4 kg at baseline. All procedures were conducted in compliance with the Animal Welfare Act Regulations (9 CFR 3).

Study Design and Dosing Schedule

All dosing and sample collections were conducted at Covance Laboratories. Individual doses of nemvaleukin were calculated based on body weight, as measured on the day of dosing in the single-dose study, and the first day of dosing in the repeat-dose study. Animals were not fasted prior to dosing. In the single-dose study, nemvaleukin was administered intravenously at 0.3 mg/kg or subcutaneously at 0.3 or 1.0 mg/kg (three animals per dose group; Supplemental Fig. 1A). In the repeat-dose study, nemvaleukin was administered intravenously at 0.1 mg/kg once daily for 5 consecutive days on days 1–5 (Group 1) or subcutaneously at 0.5 mg/kg on day 1 and day 4 (Group 2; three animals per dose group; Supplemental Fig. 1B). The i.v. dose was administered via a saphenous vein using a needle and catheter set as a slow push (over ≥1 minute). The s.c. dose was administered via syringe and needle in the mid-scapular region. Blood samples to determine serum concentrations of nemvaleukin and selected cytokines (approximately 2 ml) were collected from the femoral vein into tubes without anticoagulant at predefined time points (Supplemental Fig. 1). Whole blood samples for immunophenotyping (approximately 2 ml) were collected into tubes containing potassium EDTA anticoagulant at predefined time points (Supplemental Fig. 1).

Pharmacokinetic Data Analysis

Serum concentrations of nemvaleukin were analyzed by an independent bioanalytic laboratory (Covance, Chantilly, VA) via electrochemiluminescence assay using a sandwich immunoassay format on the Meso Scale Discovery (MSD; Meso Scale Diagnostics, LLC, Rockville, MD) platform. The capture antibody, anti-human IL-2 Rα

monoclonal antibody (Mab; Clone 24204, mouse IgG1, Cat No. MAB623, R&D Systems Inc., Minneapolis, MN), was coated onto a single-spot 96-well standard bind MSD plate and incubated for at least 12 hours at 2–8°C. The plate was washed and blocked before samples were added. Nemvaleukin in the sample was bound to the capture antibody immobilized on the working electrode surface and was detected using the SULFO-TAG™ anti-hIL-2 antibody, MAB202 (R&D Systems Inc. Cat No. MAB202 clone #5334). After a 1-hour incubation, the plates were washed and MSD Read Buffer (Meso Scale Diagnostics) added. The plate was read in an MSD Sector™ Imager 6000 (Meso Scale Diagnostics) instrument, and data were analyzed using a five-parameter logistic function with $1/y^2$ weighting in Watson software version 7.4.1 (range of quantitation 1–15 ng/ml; Thermo Scientific). The assay had a lower limit of quantitation (LLOQ) of 1.0 ng/mL and an upper limit of quantitation (ULOQ) of 15.0 ng/ml. Precision and accuracy of the assay were evaluated by analyzing quality control (QC) samples at the LLOQ (1.0 ng/mL), low QC (2.5 ng/mL), medium QC (5.0 ng/mL), high QC (11.0 ng/mL), and ULOQ (15.0 ng/ml). Please refer to the Supplemental Methods for the validation data. Nemvaleukin was stable in monkey serum for up to 26 hours at room temperature and up to six freeze/thaw cycles, for up to 72 hours refrigerated at 2–8°C, and for 3 months (99 days) at –60°C to –80°C.

PK parameters of nemvaleukin were calculated by a standard noncompartmental analysis method using Phoenix WinNonlin v6.4 (Pharsight, a Certara Company, Mountain View, CA). The following parameters were estimated after single-dose administration of nemvaleukin: maximum observed serum concentration (C_{max}), time to C_{max} (T_{max}), terminal elimination half-life ($t_{1/2}$), area under the concentration-time curve

from time 0 to the time of the last measurable serum concentration estimated by the linear trapezoidal rule (AUC_t), AUC from time 0 to infinity (AUC_∞; calculated as $AUC_\infty = AUC_t + C_t/\lambda z$, where C_t is the last measurable serum concentration and λz is the terminal elimination rate constant estimated using log-linear regression of the terminal elimination phase of the concentration-time curve), mean residence time (MRT; calculated as $AUMC_\infty/AUC_\infty$, where $AUMC_\infty$ is the area under the moment curve from 0 to infinity), total body clearance (CL; calculated as dose/AUC_∞), volume of distribution at steady state (Vd_{ss}; calculated as [$AUMC_\infty/AUC_\infty$] × CL), and absolute bioavailability after s.c. administration (%F, calculated as [(mean $AUC_{\infty(s.c.)}$ × $dose_{(i.v.)}$)/(mean $AUC_{\infty(i.v.)}$ × $dose_{(s.c.)}$)] × 100).

The following PK parameters were estimated after repeat-dose administration of nemvaleukin: C_{max}, T_{max}, $t_{1/2}$, AUC_t, and total AUC over the entire dosing period (AUC_{total}). For s.c. dosing, this was calculated as $AUC_{72h,day\ 1} + AUC_{t,day\ 4}$, and for i.v. dosing this was estimated to lie between AUC_{total} ($AUC_{24h,day\ 1}$ × 4 + $AUC_{t,day\ 5}$ [assuming AUC_{24h} on days 2, 3, and 4 = AUC_{24h} on day 1]) and AUC_{total} ($AUC_{24h,day\ 1} + AUC_{24h,day\ 5}$ × 3 + $AUC_{t,day\ 5}$ [assuming AUC_{24h} on days 2, 3, and 4 = AUC_{24h} on day 5]).

Immune Cell Analyses by Flow Cytometry

Assessment of Nemvaleukin in Vitro Potency on Primary Leukocytes. Leukocytes obtained from cynomolgus monkey whole blood after standard red blood cell lysis were counted, resuspended in X-VIVO 10 media, plated, and incubated in the presence of decreasing concentrations of nemvaleukin (4-fold dilutions beginning at 150 nM for samples intended for analysis of memory $CD8^+$ T cells and 3-fold dilutions beginning at

20 nM for samples intended for analysis of CD4$^+$ T$_{regs}$ and NK cells). Samples were stimulated or unstimulated, for approximately 30 minutes in a 37°C, 5% CO$_2$ environment. Following stimulation, cells were fixed, washed, Fc-blocked, and stained with fluorescently conjugated antibodies specific for CD4$^+$ T$_{reg}$, NK cell, or memory CD8$^+$ T cell surface markers. After surface marker staining, cells were washed and permeabilized for subsequent intracellular staining steps before sample acquisition on a BD LSRFortessa X20 (BD Biosciences, San Jose, CA). Antibodies and fluorescent dyes used are described in Supplemental Table 1. Markers used to identify immune cell populations are detailed in Supplemental Table 2.

Immunophenotyping of Whole Blood

Blood sample processing, and immunophenotypic data acquisition was performed at Alkermes, Inc. (Waltham, MA) approximately 24 hours after sample collection. Leukocytes obtained from cynomolgus monkey whole blood after standard red blood cell lysis were counted, resuspended in X-VIVO 10 media, and plated. Cells were then resuspended in viability stain buffer and incubated at room temperature, washed, Fc-blocked, and surface-stained with fluorescently conjugated antibodies. Cells were washed and permeabilized for subsequent intracellular staining steps prior to sample acquisition on a BD LSRFortessa X-20 using a high-throughput sampler. Antibodies and fluorescent dyes used are listed in Supplemental Table 3. CD4$^+$ T$_{regs}$, NK, and naïve/memory CD4$^+$ and CD8$^+$ T cell populations were identified using the markers described in Supplemental Table 4.

Quantification of Serum Concentrations of Proinflammatory Cytokines

The V-PLEX Proinflammatory Panel 1 NHP Kit (Meso Scale Diagnostics) was used to quantify concentrations of IL-1β, IL-6, IL-8, IL-10, and interferon-ɣ (IFNɣ) in monkey serum samples using an MSD SQ120 instrument.

Results

In Vitro Potency of Nemvaleukin on Activating Lymphocyte Populations

The in vitro potency of nemvaleukin on activating selected lymphocyte subsets, including CD16$^+$ NK cells, memory subsets of CD8$^+$ T cells, and CD4$^+$ T$_{regs}$, in terms of the half-maximal effective concentration (EC$_{50}$), were similar between cynomolgus monkeys and humans (Table 1), suggesting that cynomolgus monkey is a pharmacologically relevant species for predicting immunologic activity in humans. Potencies for NK cells and T$_{regs}$ were similar to each other and between the monkey and human samples, with EC$_{50}$ values within the 0.5 nM range, while EC$_{50}$ values for memory CD8$^+$ T cell subsets were in the 1–2 nM range.

Pharmacokinetics of Nemvaleukin after Single-Dose Administration

After a single i.v. bolus dose of 0.3 mg/kg, serum nemvaleukin concentrations declined in a multiexponential manner, with a mean terminal t$_{½}$ of 49.5 hours and MRT of 12.8 hours (Fig. 2A, Table 2). The mean serum CL and mean Vd$_{ss}$ were 10.6 ml/h/kg and 135 ml/kg, respectively (Table 2). After a single s.c. dose of 0.3 mg/kg or 1 mg/kg, serum concentrations of nemvaleukin peaked at 8 hours at both dose levels (Fig. 2A,

Table 2). Systemic exposure to nemvaleukin, as measured by C_{max} and AUC_∞, increased in a less than dose-proportional manner from 0.3 mg/kg to 1.0 mg/kg (Table 2). As a result, s.c. bioavailability was estimated to be 45% at 0.3 mg/kg and 28% at 1.0 mg/kg of nemvaleukin.

Pharmacokinetics of Nemvaleukin after Repeat-Dose Administration

After s.c. administration of nemvaleukin at 0.5 mg/kg, C_{max} of nemvaleukin was reached at 8 hours after the first dose on day 1 and at 2 or 8 hours after the second dose on day 4. Although peak serum concentrations of nemvaleukin after s.c. doses of 0.5 mg/kg were two- to three-fold lower than those after repeated i.v. doses of 0.1 mg/kg, trough serum concentrations and total systemic exposure to nemvaleukin (AUC_{total}) after two s.c. doses of 0.5 mg/kg (on days 1 and 4) were comparable to those after five daily i.v. doses of 0.1 mg/kg (on days 1–5; Fig. 2B, Table 3).

Pharmacodynamic Effects of Nemvaleukin

Repeat doses of i.v. and s.c. nemvaleukin resulted in notable increases in CD8^{+} T cells and NK cells, peaking on days 6–8, while only modest increases in CD4^{+} T_{regs} were observed (Fig. 3A and 3B). Elevated numbers of CD8^{+} T cells and CD56^{+} NK cells were sustained until day 14, at which point cell numbers returned to predose levels. The expansion of CD8^{+} T cells and CD56^{+} NK cells was similar between the two dosing regimens, with six- and four-fold increases, respectively. In contrast, approximately two-fold increases in CD4^{+} T_{regs} were observed (Fig. 3B). Expression of the intracellular proliferation marker Ki-67 was also measured. Increased expression of Ki-67 was observed starting on day 3, and peaked at greater than 80% on day 6 for CD8^{+} T cells

and CD56$^+$ NK cells after i.v. administration (Fig. 3C). The peak of Ki-67 expression was not captured following s.c. administration because several blood samples collected on days 6 and 7 froze during shipment, precluding their analyses. Increased Ki-67 expression was also observed in CD4$^+$ T$_{regs}$, but to a lesser extent (~40%), consistent with the modest two-fold increases in cell numbers.

To assess whether particular subsets of CD8$^+$ T cells responded more markedly to nemvaleukin, CD8$^+$ T cells were categorized as naïve, central memory, effector memory, and terminal effector phenotype CD8$^+$ populations according to the surface markers listed in Supplemental Table 4. Increased cell numbers following i.v. and s.c. administration of nemvaleukin were observed for all CD8$^+$ T cell subsets (Fig. 4A). Numbers of terminal effector and effector memory CD8$^+$ T cells were increased to a greater extent than of central memory and naïve CD8$^+$ T cells, by approximately 20- and 30-fold compared with 10- and 4-fold, respectively (Fig. 4B).

Changes in the number of central memory CD4$^+$ T cells following repeat-dose administration of nemvaleukin (Supplemental Fig. 2) were generally similar to the observed changes in CD4$^+$ T$_{regs}$.

Serum levels of proinflammatory cytokines were also measured, and may correlate with responses by particular immune cell populations. Transient elevation of IL-6 and IFNɣ was observed following both i.v. and s.c. administration of ALKS 4320 and peaked at 2 hours (i.v.) and 8 hours (s.c.) post dosing (Supplemental Fig. 3). No notable increases in levels of IL-1β, IL-8, or IL-10 were observed following i.v. or s.c. administration of nemvaleukin (data not shown).

Discussion (1500-word limit; currently at 954)

The amplification of antitumor T cell responses is a key component of the cancer immunity cycle and forms the basis of the rationale for the use of high-dose IL-2 in patients with metastatic melanoma or advanced renal cell carcinoma (Chen and Mellman, 2013; Clark et al., 2017; Buchbinder et al., 2019; Fishman et al., 2019). However, high-dose IL-2 therapy has been shown to induce expansion of both antitumor effector cell and T_{reg} populations, with greater expansion of $ICOS^+ T_{regs}$ correlating with poor outcome of high-dose IL-2 therapy (Sim et al., 2014). In addition, maximal efficacy of recombinant IL-2 therapy in humans requires an intensive high-dose i.v. administration regimen, as demonstrated in a head-to-head phase III study comparing i.v. dosing regimens (McDermott et al., 2015). Nemvaleukin is designed to selectively activate antitumor T cell and NK cell populations over T_{regs}, as was observed in mice and with human peripheral blood mononuclear cells in vitro. In addition, equivalent antitumor efficacy was observed following i.v. and s.c. administration of nemvaleukin in tumor-bearing mice (Lopes et al., 2020). The pathological effects of recombinant IL-2 in monkeys are known to be predictive of pathogenesis in humans (Harada and Yahara, 1993; Gillies et al., 2011). As the in vitro potency for nemvaleukin on immune cell subsets found in peripheral blood were similar for cynomolgus monkeys and humans, the PK-PD relationship in cynomolgus monkeys is expected to inform dose selection and predict PD effects in humans. These studies conducted with cynomolgus monkeys set out to compare the PK and PD effects of single or repeated doses of nemvaleukin following i.v. or s.c. administration. An additional goal was to ascertain whether s.c. administration of nemvaleukin could achieve similar or more favorable PD responses versus i.v. administration in cynomolgus monkeys.

PK analysis showed that s.c. administration of nemvaleukin with less frequent dosing can achieve total systemic exposure and trough serum concentrations that are comparable to those achieved with daily i.v. administration, albeit with lower peak serum concentrations. Analysis of the PD effects of nemvaleukin on multiple immune cell subtypes (including circulating $CD4^+$ T cells, $CD8^+$ T cells, $CD56^+$ NK cells, and T_{regs}) revealed the selective expansion of potentially immunoprotective central memory, effector memory, and terminal effector $CD8^+$ T cell and $CD56^+$ NK cell populations following both i.v. and s.c. administration. It is worth noting that in the current study, the overall expansion of $CD8^+$ T cell and NK cell populations was similar between i.v. (once daily on days 1–5) and s.c. (on day 1 and day 4) dosing regimens, which correlated with similar total systemic exposure to nemvaleukin between the two dosing regimens.

Ki-67 protein expression was used as a marker of immune cell proliferation and, as such, has been validated and is widely used as a means of quantifying the dividing fraction of a given cell population (Scholzen and Gerdes, 2000; Sun and Kaufman, 2018). Our data show that the expanded populations of $CD8^+$ T cells and NK cells that result from nemvaleukin administration are actively undergoing proliferation, while the population of T_{regs} showed less pronounced levels of proliferation. The comparatively modest expansion of total T_{regs} following administration of i.v. or s.c. nemvaleukin further supports its immunotherapeutic potential and distinguishes it from other IL-2–based therapies. The selective expansion of $CD8^+$ T cells and NK cells by nemvaleukin, with limited impact on T_{reg} expansion, observed in mice (Lopes et al., 2020) and here in cynomolgus monkeys, is in marked contrast to the T_{reg}-biased immune profile induced by recombinant IL-2 in mice (Lopes et al., 2020), monkeys (Bell et al., 2015), and

Confidential draft   Page | 17

humans (Sim et al., 2014). Indeed, the propensity of low-dose recombinant IL-2 to elicit the expansion of T_{regs} has prompted its use as a treatment for autoimmune diseases, such as rheumatoid arthritis, which are characterized by deficiencies of T_{regs} (Ye et al., 2018).

Analysis of serum concentrations of proinflammatory cytokines showed transient elevation of both IL-6 and IFNɣ that peaked at 2 hours and 8 hours after i.v. and s.c. administration of nemvaleukin, respectively. After repeat dosing, levels of IL-6 trended higher following i.v. administration relative to s.c. administration, which could be attributed to the higher observed C_{max} for nemvaleukin after i.v. administration compared with s.c. administration. These cytokine data might suggest better tolerability with an s.c. treatment regimen, given the association between IL-6 and loss of endothelial barrier function and, by implication, vascular leakage (Alsaffar et al., 2018; Narazaki and Kishimoto, 2018). IFNɣ production by immune effector cells is associated with antitumor efficacy (Ivashkiv, 2018); therefore, the induction of IFNɣ suggests that nemvaleukin might promote the activation of cells associated with antitumor immune responses following both i.v. and s.c. administration.

In conclusion, s.c. administration of nemvaleukin can achieve total systemic exposure similar to that of i.v. administration, with less frequent dosing and a lower C_{max}, resulting in similar expansion of CD8^{+} T cells and CD56^{+} NK cells with minimal expansion of CD4^{+} T_{regs}. The PK and PD data in monkeys reported here support clinical evaluation of i.v. and s.c. administration of nemvaleukin in humans with advanced solid tumors. In addition to the ongoing phase I/II ARTISTRY-1 first-in-human study of i.v. nemvaleukin (NCT02799095), the PD, PK, safety, and efficacy of s.c.

Confidential draft   Page | 18

administration of nemvaleukin are currently under investigation in the phase I/II

ARTISTRY-2 study (NCT03861793). The selection of s.c. nemvaleukin dose and dosing

frequency in ARTISTRY-2 was determined from predictions (manuscript in

development) based on the observed PK-PD relationship from ARTISTRY-1 and in

monkeys after i.v. and s.c. routes of administration. In the ARTISTRY-2 study, s.c.

nemvaleukin is given as a single agent or in combination with pembrolizumab to

patients with selected advanced or metastatic solid tumors. The s.c. route of

administration might provide an alternative administration option for patients.

ACKNOWLEDGMENTS

DECLARATIONS

Availability of data and material: The datasets used and/or analyzed during the current study are available from the corresponding author upon reasonable request.

Disclosures and Conflicts of Interest: Lei Sun, Jared E. Lopes, Heather L. Flick, Erin A. Murphy, and Heather C. Losey are employees and stockholders of Alkermes, Inc.

Author contributions:

Participated in research design: Lopes, Sun, and Losey

Conducted experiments: Lopes, Sun, Flick, and Murphy

Contributed new reagents or analytic tools: Lopes, Sun, Flick, Murphy, and Losey

Performed data analysis: Lopes, Sun, Flick, Murphy, and Losey

Wrote or contributed to the writing of the manuscript: Lopes, Sun, Flick, Murphy, and Losey

REFERENCES

Ahmadzadeh M, and Rosenberg SA (2006) IL-2 administration increases CD4+ CD25(hi) Foxp3+ regulatory T cells in cancer patients. *Blood* **107**:2409-2414.

Alsaffar H, Martino N, Garrett JP, and Adam AP (2018) Interleukin-6 promotes a sustained loss of endothelial barrier function via Janus kinase-mediated STAT3 phosphorylation and de novo protein synthesis. *Am J Physiol Cell Physiol* **314**:C589-C602.

Amaria RN, Reuben A, Cooper ZA, and Wargo JA (2015) Update on use of aldesleukin for treatment of high-risk metastatic melanoma. *Immunotargets Ther* **4**:79-89.

Antony PA, and Restifo NP (2005) CD4+CD25+ T regulatory cells, immunotherapy of cancer, and interleukin-2. *J Immunother* **28**:120-128.

Atkins MB, Lotze MT, Dutcher JP, Fisher RI, Weiss G, Margolin K, Abrams J, Sznol M, Parkinson D, Hawkins M, Paradise C, Kunkel L, and Rosenberg SA (1999) High-dose recombinant interleukin 2 therapy for patients with metastatic melanoma: analysis of 270 patients treated between 1985 and 1993. *J Clin Oncol* **17**:2105-2116.

Bell CJ, Sun Y, Nowak UM, Clark J, Howlett S, Pekalski ML, Yang X, Ast O, Waldhauer I, Freimoser-Grundschober A, Moessner E, Umana P, Klein C, Hosse RJ, Wicker LS, and Peterson LB (2015) Sustained in vivo signaling by long-lived IL-2 induces prolonged increases of regulatory T cells. *J Autoimmun* **56**:66-80.

Boyman O, and Sprent J (2012) The role of interleukin-2 during homeostasis and activation of the immune system. *Nat Rev Immunol* **12**:180-190.

Buchbinder EI, Dutcher JP, Daniels GA, Curti BD, Patel SP, Holtan SG, Miletello GP, Fishman MN, Gonzalez R, Clark JI, Richart JM, Lao CD, Tykodi SS, Silk AW, and McDermott DF (2019) Therapy with high-dose Interleukin-2 (HD IL-2) in metastatic melanoma and renal cell carcinoma following PD1 or PDL1 inhibition. *J Immunother Cancer* **7**:49.

Chen DS, and Mellman I (2013) Oncology meets immunology: the cancer-immunity cycle. *Immunity* **39**:1-10.

Choudhry H, Helmi N, Abdulaal WH, Zeyadi M, Zamzami MA, Wu W, Mahmoud MM, Warsi MK, Rasool M, and Jamal MS (2018) Prospects of IL-2 in cancer immunotherapy. *Biomed Res Int* **2018**:9056173.

Clark JI, Wong MKK, Kaufman HL, Daniels GA, Morse MA, McDermott DF, Agarwala SS, Lewis LD, Stewart JH, Vaishampayan U, Curti B, Gonzalez R, Lutzky J, Rudraptna V, Cranmer LD, Jeter JM, Hauke RJ, Miletello G, Milhem MM, Amin A, Richart JM, Fishman M, Hallmeyer S, Patel SP, Van Veldhuizen P, Agarwal N, Taback B, Treisman JS, Ernstoff MS, Perritt JC, Hua H, Rao TB, Dutcher JP, and Aung S (2017) Impact of sequencing targeted therapies with high-dose interleukin-2 immunotherapy: an analysis of outcome and survival of patients with metastatic renal cell carcinoma from an on-going observational IL-2 clinical trial: PROCLAIM(SM). *Clin Genitourin Cancer* **15**:31-41 e34.

Fishman M, Dutcher JP, Clark JI, Alva A, Miletello GP, Curti B, Agarwal N, Hauke R, Mahoney KM, Moon H, Treisman J, Tykodi SS, Daniels G, Morse MA, Wong MKK, Kaufman H, Gregory N, and McDermott DF (2019) Overall survival by clinical risk category for high dose interleukin-2 (HD IL-2) treated patients with metastatic renal

cell cancer (mRCC): data from the PROCLAIM(SM) registry. *J Immunother Cancer* **7**:84.

Gillies SD, Lan Y, Hettmann T, Brunkhorst B, Sun Y, Mueller SO, and Lo KM (2011) A low-toxicity IL-2-based immunocytokine retains antitumor activity despite its high degree of IL-2 receptor selectivity. *Clin Cancer Res* **17**:3673-3685.

Harada Y and Yahara I (1993) Pathogenesis of toxicity with human-derived interleukin-2 in experimental animals. *Int Rev Exp Pathol* **34 Pt A**:37-55.

Ivashkiv LB (2018) IFNgamma: signalling, epigenetics and roles in immunity, metabolism, disease and cancer immunotherapy. *Nat Rev Immunol* **18**:545-558.

Lopes JE, Fisher JL, Flick HL, Wang C, Sun L, Ernstoff MS, Alvarez JC, and Losey HC (2020) ALKS 4230: a novel engineered IL-2 fusion protein with an improved cellular selectivity profile for cancer immunotherapy. *J Immunother Cancer* **8**.

McDermott DF, Cheng SC, Signoretti S, Margolin KA, Clark JI, Sosman JA, Dutcher JP, Logan TF, Curti BD, Ernstoff MS, Appleman L, Wong MK, Khushalani NI, Oleksowicz L, Vaishampayan UN, Mier JW, Panka DJ, Bhatt RS, Bailey AS, Leibovich BC, Kwon ED, Kabbinavar FF, Belldegrun AS, Figlin RA, Pantuck AJ, Regan MM, and Atkins MB (2015) The high-dose aldesleukin "select" trial: a trial to prospectively validate predictive models of response to treatment in patients with metastatic renal cell carcinoma. *Clin Cancer Res* **21**:561-568.

Narazaki M and Kishimoto T (2018) The two-faced cytokine IL-6 in host defense and diseases. *Int J Mol Sci* **19**.

Scholzen T and Gerdes J (2000) The Ki-67 protein: from the known and the unknown. *J Cell Physiol* **182**:311-322.

Sim GC, Martin-Orozco N, Jin L, Yang Y, Wu S, Washington E, Sanders D, Lacey C, Wang Y, Vence L, Hwu P, and Radvanyi L (2014) IL-2 therapy promotes suppressive ICOS+ Treg expansion in melanoma patients. *J Clin Invest* **124**:99-110.

Skrombolas D and Frelinger JG (2014) Challenges and developing solutions for increasing the benefits of IL-2 treatment in tumor therapy. *Expert Rev Clin Immunol* **10**:207-217.

Sun X and Kaufman PD (2018) Ki-67: more than a proliferation marker. *Chromosoma* **127**:175-186.

Sun Z, Ren Z, Yang K, Liu Z, Cao S, Deng S, Xu L, Liang Y, Guo J, Bian Y, Xu H, Shi J, Wang F, Fu YX, and Peng H (2019) A next-generation tumor-targeting IL-2 preferentially promotes tumor-infiltrating CD8(+) T-cell response and effective tumor control. *Nat Commun* **10**:3874.

Waldmann TA (2006) The biology of interleukin-2 and interleukin-15: implications for cancer therapy and vaccine design. *Nat Rev Immunol* **6**:595-601.

Ye C, Brand D, and Zheng SG (2018) Targeting IL-2: an unexpected effect in treating immunological diseases. *Signal Transduct Target Ther* **3**:2.

Confidential draft

FOOTNOTES

[1]Co-primary authors

[2]Corresponding author

FIGURE LEGENDS

Fig. 1. Mechanism of action of nemvaleukin. (A) Visualization of spatial distance between unfused IL-2 and IL-2R (with native N-termini and C-termini labeled). (B) Nemvaleukin selectively engages the intermediate-affinity IL-2R complex that is expressed on subsets of CD8$^+$ T cells and NK cells and is sterically occluded from binding to the high-affinity IL-2R complex that is expressed on CD4$^+$ T$_{regs}$.

Fig. 2. Mean (+ SD) serum concentrations (ng/ml) of nemvaleukin in male cynomolgus monkeys after (A) single i.v. (0.3 mg/kg) or s.c. doses (0.3, 1.0 mg/kg) and (B) repeated i.v. (0.1 mg/kg for 5 consecutive days, on days 1–5) or s.c. doses (0.5 mg/kg on days 1 and 4). N = 3 per treatment group.

Fig. 3. Effect of repeated i.v. (0.1 mg/kg for 5 consecutive days) or s.c. (0.5 mg/kg on days 1 and 4) administration of nemvaleukin on (A) total CD8$^+$ T cells and CD56$^+$ NK cells and (B) CD4$^+$ T$_{regs}$, and (C) the proportion of cells expressing the cell proliferation marker Ki-67. Data shown are the mean ± standard error of the mean (SEM) with N = 3 per treatment group. Fold changes were calculated relative to predose levels for individual monkeys.

Fig. 4. Effect of repeated i.v. (0.1 mg/kg for 5 consecutive days) or s.c. (0.5 mg/kg on days 1 and 4) administration of nemvaleukin on CD8$^+$ T cell subsets in terms of (A) cell numbers and (B) fold change relative to predose levels. Data shown are the mean ± SEM with N = 3 per treatment group.

TABLES

TABLE 1

Potency of nemvaleukin on selected lymphocyte subsets from cynomolgus monkey and human samples (Lopes et al., 2020)

Lymphocyte Population	Monkey EC_{50} (nM) Mean ± SD	Human[a] EC_{50} (nM) Mean ± SD
NK cells	0.47 ± 0.22	0.45 ± 0.09
Naïve $CD8^+$ T cells	1.4 ± 0.3	2.2 ± 1.0
Central/transitional memory $CD8^+$ T cells	1.3 ± 0.4	1.1 ± 0.1
Effector memory $CD8^+$ T cells	2.0 ± 1.0	1.25 ± 0.4
Terminal effector $CD8^+$ T cells	1.7 ± 0.8	0.93 ± 0.3
T_{regs}	0.50 ± 0.14	0.59 ± 0.2

[a]Data generated from three separate experiments, each performed in triplicate, and the error represents SD.

SD, standard deviation.

TABLE 2

PK parameters of nemvaleukin in male cynomolgus monkeys after a single i.v. (0.3 mg/kg) or s.c. (0.3 or 1.0 mg/kg) dose

Dose Route	Dose (mg/kg)	C_{max} (ng/ml)	T_{max} (h)	AUC_∞ (ng·h/ml)	$t_{1/2}$ (h)	MRT (h)	CL (ml/h/kg)	Vd_{ss} (ml/kg)
Intravenous	0.3	6119 ± 1188	0.083 (0.083, 0.083)	28,460 ± 1230	49.5 ± 5.6	12.8 ± 1.9	10.6 ± 0.46	135 ± 16.6
Subcutaneous	0.3	549 ± 208	8 (8, 8)	12,931 ± 3893	61.9 ± 4.6	31.6 ± 4.0	—	—
Subcutaneous	1.0	1035 ± 133	8 (8, 8)	26,878 ± 2106	37.3 ± 19.4	21.7 ± 2.8	—	—

N = 3 per treatment group.

Mean (± SD) for all parameters except T_{max} [median (min, max)].

TABLE 3

PK parameters of nemvaleukin in male cynomolgus monkeys after repeated i.v. (0.1 mg/kg for 5 consecutive days, on days 1–5) or s.c. (0.5 mg/kg on days 1 and 4) doses

Dose route	Dose (mg/kg)	Day	C_{max} (ng/ml)	T_{max} (h)	C_{trough} (ng/ml)	AUC_τ[a] (ng·h/ml)	AUC_t (ng·h/ml)	AUC_{total} (ng·h/ml)
Intravenous	0.1	1	2575 ± 176	0.083 (0.083, 0.083)	<LLOQ	9035 ± 602	9035 ± 602	41,753 ± 2213[b]
		5	2096 ± 80	0.083 (0.083, 0.083)	9.62 ± 1.39	5159 ± 301	5611 ± 429	30,124 ± 1112[c]
Subcutaneous	0.5	1	911 ± 432	8 (8, 8)	<LLOQ	17,656 ± 6700	17,656 ± 6700	33,402 ± 9204
		4	1006 ± 119	2 (2, 8)	10.0 ± 1.25	15,214 ± 2529	15,746 ± 2601	

N = 3 per treatment group. LLOQ: lower limit of quantitation (1.00 ng/mL)

Confidential draft

Mean (± SD) for all parameters except T_{max} [median (min, max)].

[a] τ = 24 hours for i.v. dosing regimen and 72 hours for s.c. dosing regimen.

[b] Calculated based on $AUC_{24h,day\ 1} \times 4 + AUC_{t,day\ 5}$.

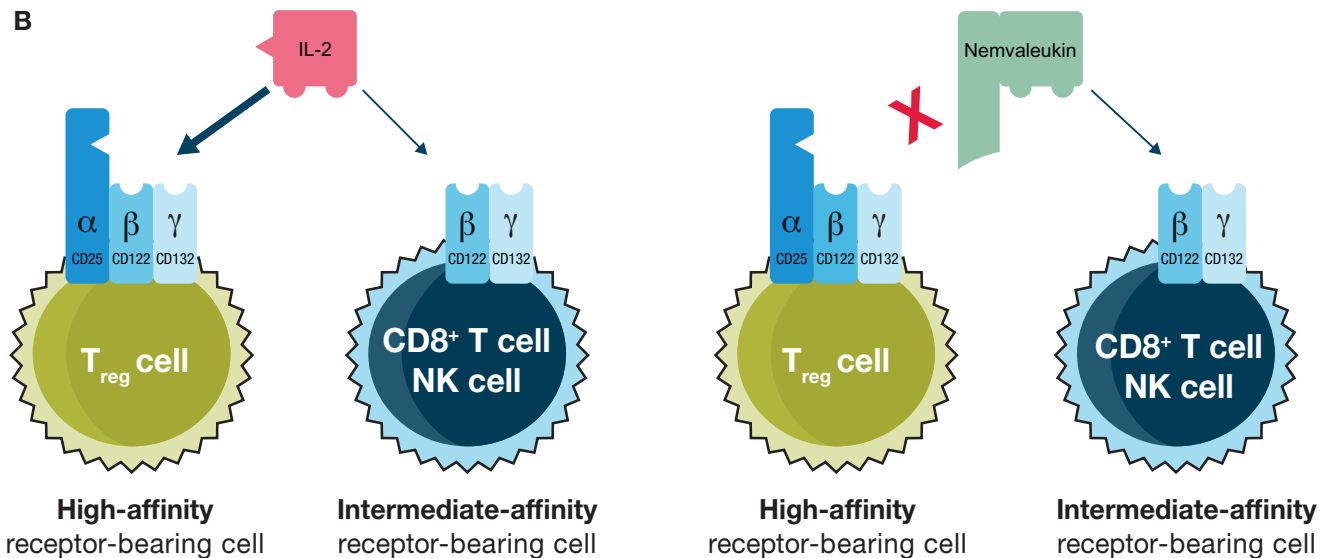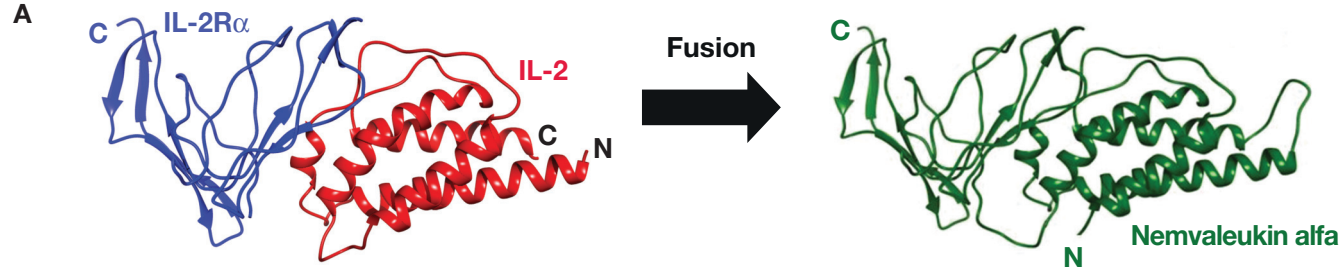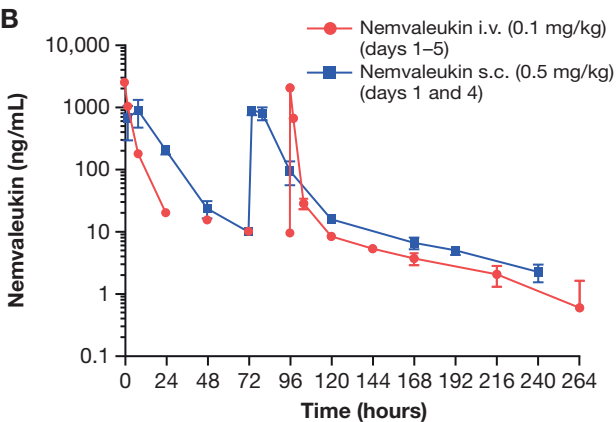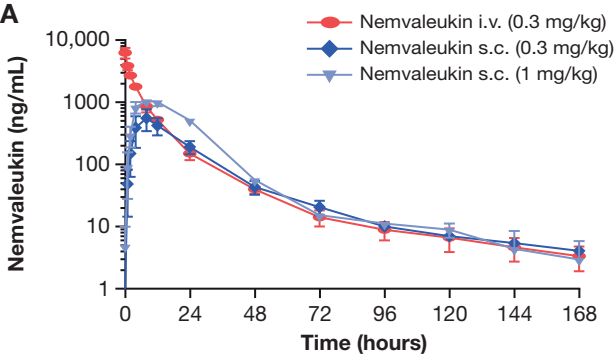[c] Calculated based on $AUC_{24h,day\ 1} + AUC_{24h,day\ 5} \times 3 + AUC_{t,day\ 5}$.

Figure 1

Figure 2

Figure 3

A

Naïve CD8 T Cells

Central Memory CD8 T Cells

Effector Memory CD8 T Cells

Terminal Effector CD8 T Cells

B

Naïve Memory CD8 T Cells Fold Change

Central Memory CD8 T Cells Fold Change

Effector Memory CD8 T Cells Fold Change

Terminal Effector CD8 T Cells Fold Change

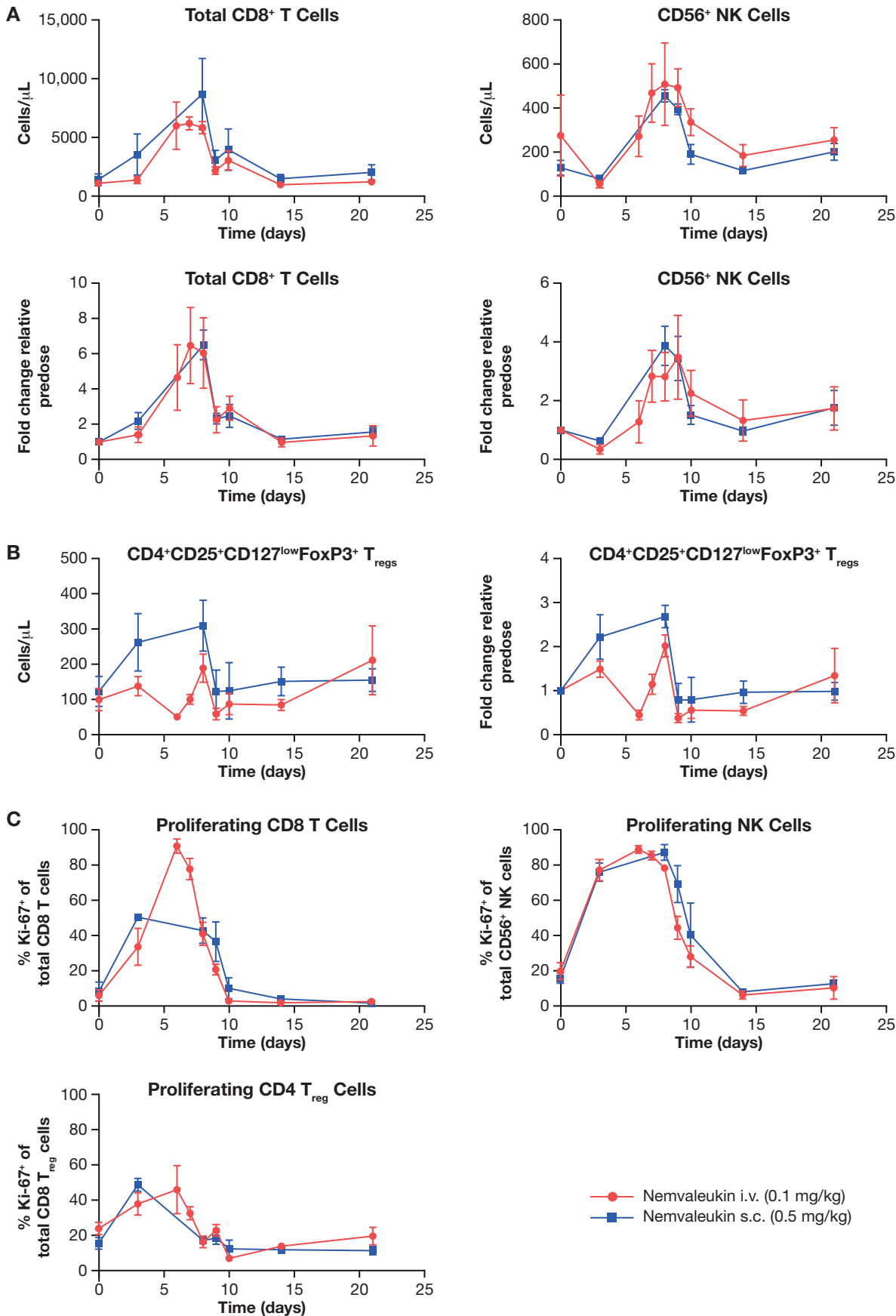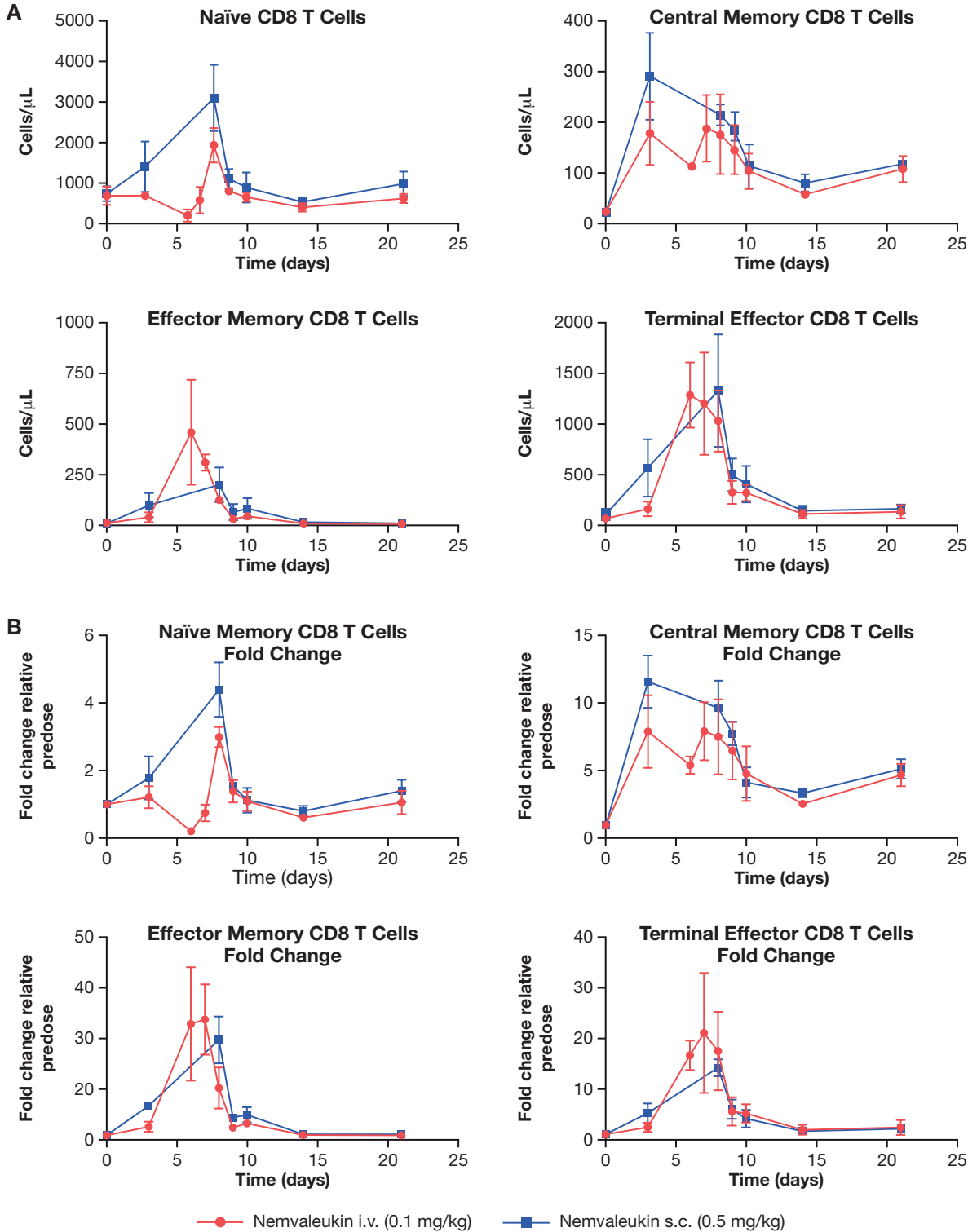Nemvaleukin i.v. (0.1 mg/kg)   Nemvaleukin s.c. (0.5 mg/kg)

Figure 4

SUPPLEMENTAL MATERIALS

Pharmacokinetics and Pharmacodynamic Effects of Nemvaleukin Alfa, a Selective Agonist of the Intermediate-Affinity IL-2 Receptor, in Cynomolgus Monkeys

Jared E. Lopes, Lei Sun, Heather L. Flick, Erin A. Murphy, and Heather C. Losey

Journal of Pharmacology and Experimental Therapeutics

Supplemental Methods

The pharmacokinetic assay was validated by evaluating its precision and accuracy. Precision was expressed as the percentage of coefficient of variation (%CV) of each quality control (QC) concentration. The mean inter-assay (between run) precision (%CV) for the low QC, medium QC, and high QC ranged from 8.0% to 12.8% and achieved the targeted acceptance criterion of %CV <20%. The mean inter-assay precision (%CV) for the lower limit of quantitation (LLOQ) and upper limit of quantitation (ULOQ) ranged from 7.4% to 15.1% and achieved the targeted acceptance criterion of %CV <25%. The mean intra-assay (within run) precision (%CV) for the low QC, medium QC, and high QC ranged from 0.4% to 6.4% and achieved the targeted acceptance criterion of %CV <20%. The mean inter-assay precision (%CV) for the LLOQ and ULOQ ranged from 0.8% to 6.6% and achieved the targeted acceptance criterion of %CV <25%. Accuracy was assessed as the percentage difference from the theoretical analyte concentration (%bias). The mean inter-assay accuracy (%bias) for the low QC, medium QC, and high QC ranged from 7.9% to 10.8% and achieved the targeted acceptance criterion of %bias of ±20%. The mean inter-assay accuracy (%bias) for LLOQ and ULOQ ranged from 0.8% to 12.3% and achieved the targeted acceptance criterion of %bias of ±25%. The mean intra-assay accuracy (%bias) for the low QC, medium QC, and high QC ranged from –5.9% to 24.9% and achieved the targeted acceptance criterion of %bias of ±20% for medium and high QC and for four of six runs (67%) at low QC. The mean intra-assay accuracy (%bias) for the LLOQ and ULOQ ranged from –8.7 to 28.4% and achieved the targeted acceptance criterion of %bias of ±25% for 67% of the runs.

The total error (TE) represents the overall error that may occur in a test result due to both the imprecision and inaccuracy of the measurement procedure. The mean TE for the low QC, medium QC, and high QC ranged from 15.9% to 23.6% and achieved the targeted acceptance criterion of TE <30%. The mean TE for the LLOQ and ULOQ ranged from 8.2% to 27.4% and achieved the targeted acceptance criterion of TE <40%.

Supplemental Table 1

Antibodies and fluorescent dyes used for determination of pSTAT5 levels in white blood cells from cynomolgus monkeys by flow cytometry

Antibodies/Dyes	Vendor
Anti-human CD3 V500 (clone: SP34-2)	BD Biosciences
Anti-human CD4 PE-Cy7 (clone: L200)	BD Biosciences
Anti-human CD8 APC (clone: SK1)	BioLegend
Anti-human CD14 PE-Texas Red (clone: TuK4)	Life Technologies
Anti-human CD16 BV605 (clone: 3G8)	BD Biosciences
Anti-human CD25 BV421 (clone: M-A251)	BD Biosciences
Anti-human CD28 PE (clone: 10F3)	BD Biosciences
Anti-human CD45RA APC-H7 (clone: 5H9)	BD Biosciences
Anti-human CD56 PE (clone: MY31)	BD Biosciences
Anti-human CD95 BV421 (clone: DX2)	BD Biosciences
Anti-STAT5 (pY694) Alexa Fluor 488 (clone: 47)	BD Biosciences
Anti-human FOXP3 Alexa Fluor 647 (clone: 259D)	BioLegend
Zombie NIR Fixable Dye Kit	BioLegend
Zombie Red Fixable Dye Kit	BioLegend

Supplemental Table 2

Markers used to identify immune cell subtypes for pSTAT5 analyses from cynomolgus monkeys

Cynomolgus Monkey Immune Cell Population	Gated Biomarkers
$CD4^+$ T_{regs}	$CD14^-$ $CD3^+$ $CD4^+$ $CD25^{high}$ $FoxP3^+$
NK cells	$CD14^-$ $CD3^-$ $CD16^+$
Naïve $CD8^+$ T cells	$CD14^-$ $CD3^+$ $CD8^+$ $CD28^+$ $CD45RA^+$ $CD95^-$
Central/Transitional memory $CD8^+$ T cells	$CD14^-$ $CD3^+$ $CD8^+$ $CD28^+$ $CD45RA^-$ $CD95^+$
Effector memory $CD8^+$ T cells	$CD14^-$ $CD3^+$ $CD8^+$ $CD28^-$ $CD45RA^-$ CD95+
Terminal effector $CD8^+$ T cells	$CD14^-$ $CD3^+$ $CD8^+$ $CD28^-$ $CD45RA^+$ $CD95^+$

Supplemental Table 3

Antibodies and fluorescent dyes used for phenotyping of white blood cells by flow cytometry in peripheral blood of cynomolgus monkeys

| Antibodies/Dyes	Vendor
Zombie UV Dye	BioLegend
CD127 PE-Vio770 (MB15-18C9)	Miltenyi Biotec
ICOS PerCP Cy5.5 (C398.4A)	BioLegend
Armenian Hamster IgG PerCP Cy5.5	BioLegend
CD56 PE (NCAM 16.2)	BD Biosciences
Ki-67 Alexa 488 (B56)	BD Biosciences
Mouse IgG1,k alexa 488 (MOPC-21)	BD Biosciences
CD14 APC-H7 (M5E2)	BD Biosciences
CD4 alexa 700 (L200)	BD Biosciences
FOXP3 alexa 647 (259D)	BioLegend
Mouse IgG1, k alexa 647 (MOPC-21)	BioLegend
CD16 BV605 (3G8)	BD Biosciences
CD69 BV510 (FN50)	BioLegend
Mouse IgG1, k BV510 (MOPC-21)	BioLegend
CD25 BV421 (M-A251)	BD Biosciences
Mouse IgG1, k BV421 (X40)	BD Biosciences
CD20 BUV737 (2H7)	BD Biosciences
CD3 BUV395 (SP34-2)	BD Biosciences
CCR7 PE-Cy7 (G043H7)	BioLegend

|	
CD4 PerCP Cy5.5 (L200)	BD Biosciences
CD28 PE (10F3)	ThermoFisher
CD45RA APC-H7 (5H9)	BD Biosciences
CD14 alexa 700 (M5E2)	BD Biosciences
Mouse IgG2b APC (IS6-11E5.11)	Miltenyi Biotec
CD95 BV605 (DX2)	BioLegend
CD8 BV510 (SK1)	BioLegend
Armenian Hamster IgG BV421	BioLegend

Supplemental Table 4

Markers used to identify immune cell subsets in the peripheral blood of cynomolgus monkeys

Immune Cell Population	Positively Gated Biomarkers	Negatively Gated Biomarkers
NK cells	$CD56^+$	$CD14^-$ $CD3^-$
Naïve $CD8^+$ T cells	$CD3^+$ $CD8^+$ $CD45RA^+$	$CD14^-$ $CD4^-$ $CD95^-$
Central memory $CD8^+$ T cells	$CD3^+$ $CD8^+$ $CD95^+$ $CD28^+$ $CCR7^+$	$CD14^-$ $CD4^-$ $CD45RA^-$
Effector memory $CD8^+$ T cells	$CD3^+$ $CD8^+$ $CD95^+$	$CD14^-$ $CD4^-$ $CD28^-$ $CCR7^-$ $CD45RA^-$
Terminal effector $CD8^+$ T cells	$CD3^+$ $CD8^+$ $CD95^+$ $CD45RA^+$	$CD14^-$ $CD4^-$ $CD28^-$ $CCR7^-$
Central memory $CD4^+$ T cells	$CD3^+$ $CD4^+$ $CD95^+$ $CD28^+$ $CCR7^+$	$CD14^-$ $CD8^-$ $CD45RA^-$
$CD4^+$ T_{regs}	$CD3^+$ $CD4^+$ $CD25^+$ $FoxP3^+$	$CD14^-$ $CD127^{-/low}$

Supplemental Fig. 1. Study design and dosing schedules for the (A) single- and (B) repeat-dose studies. Blood samples taken prior to dosing on each day of dose administration.
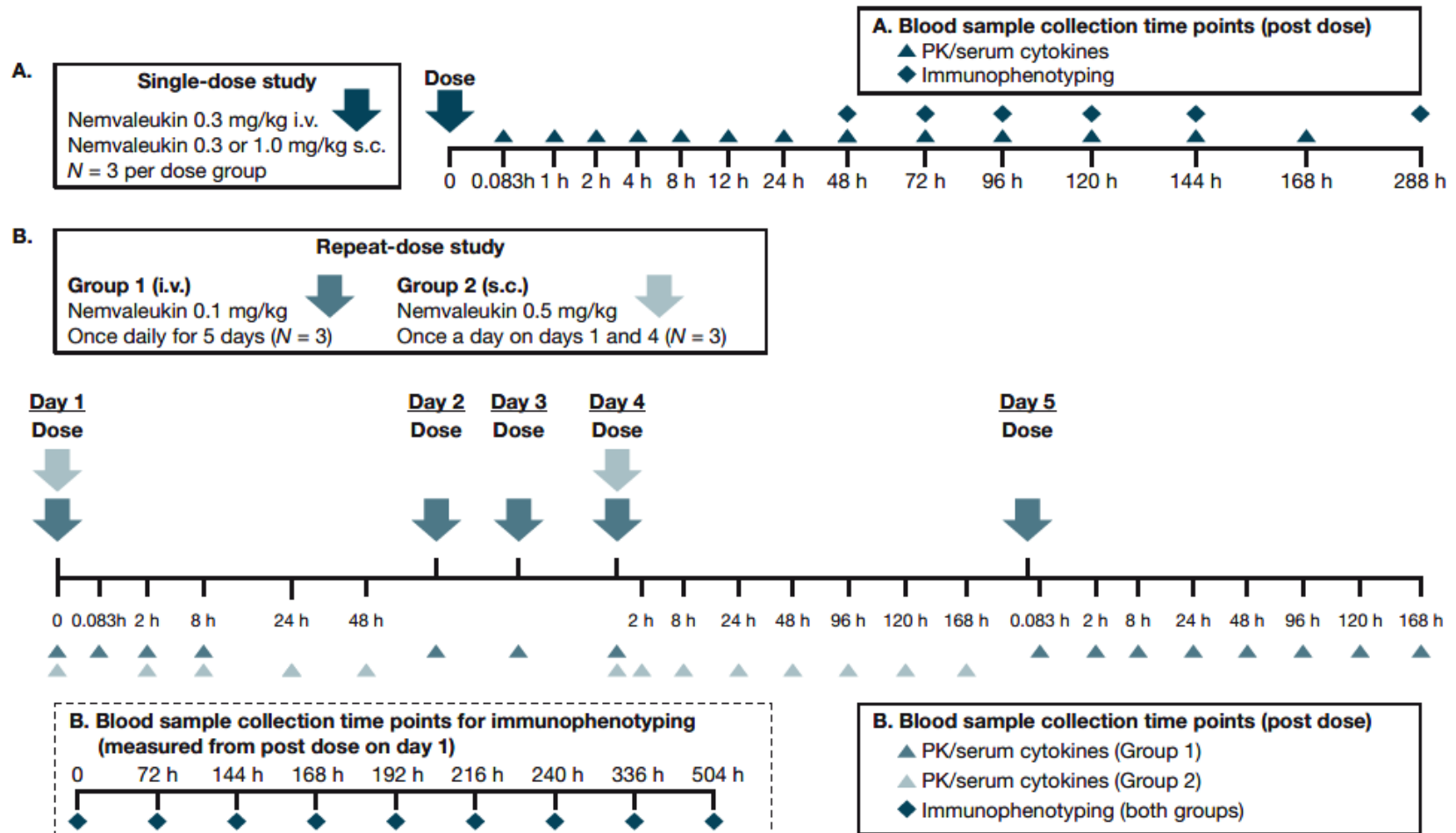
Supplemental Fig. 2. Effect of repeated i.v. (0.1 mg/kg for 5 consecutive days) or s.c. (0.5 mg/kg on days 1 and 4) administration of nemvaleukin on central memory CD4^{+} T cells and the proportion of cells expressing the cell proliferation marker Ki-67. Data shown are the mean ± standard error of the mean with $N = 3$ per treatment group.
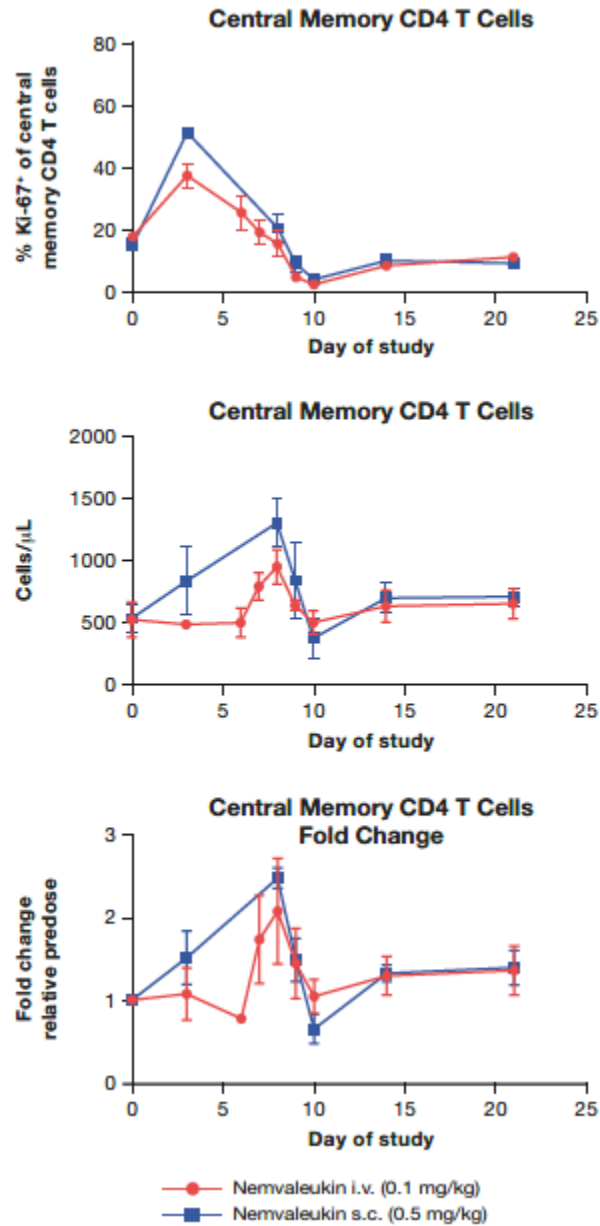
Supplemental Fig. 3. Effect of repeated i.v. (0.1 mg/kg for 5 consecutive days) or s.c. (0.5 mg/kg on days 1 and 4) administration of nemvaleukin on IL-6 and IFNγ levels. *N* = 3 per treatment group.
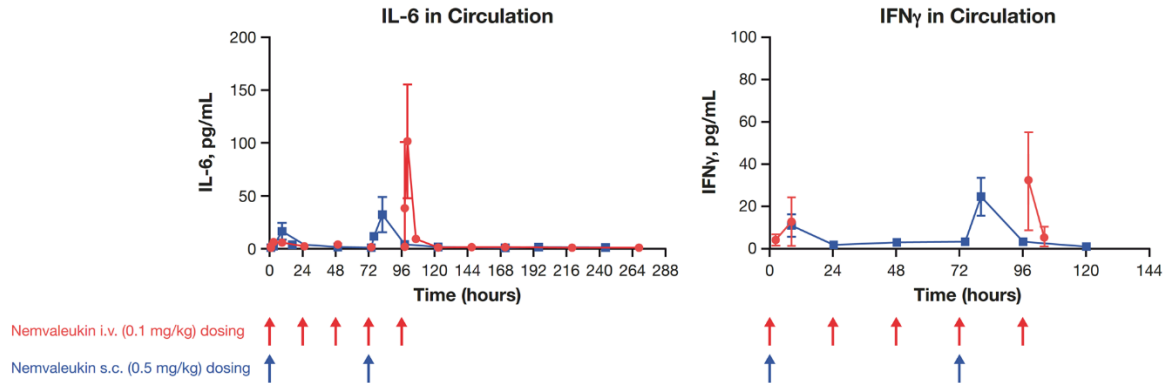
Dosing regimen	IL-6		IFNγ	
	C_{max} (pg/mL), mean ± SD (range)	T_{max} (h)	C_{max} (pg/mL), mean ± SD (range)	T_{max} (h)
Nemvaleukin i.v. (0.1 mg/kg) q.d. ×5 (on days 1–5)	102 ± 54 (42–148)	98	33 ± 24 (6–52)	98
Nemvaleukin s.c. (0.5 mg/kg) (on days 1 and 4)	32 ± 17 (13–42)	90	25 ± 15 (10–41)	90